

Provided for non-commercial research and education use.
Not for reproduction, distribution or commercial use.



This article was published in an Elsevier journal. The attached copy is furnished to the author for non-commercial research and education use, including for instruction at the author's institution, sharing with colleagues and providing to institution administration.

Other uses, including reproduction and distribution, or selling or licensing copies, or posting to personal, institutional or third party websites are prohibited.

In most cases authors are permitted to post their version of the article (e.g. in Word or Tex form) to their personal website or institutional repository. Authors requiring further information regarding Elsevier's archiving and manuscript policies are encouraged to visit:

<http://www.elsevier.com/copyright>



Preferential occupation of molybdenum on the thin alumina film: Characterization by CO titration

Zhiquan Jiang^{a,b}, Weixin Huang^b, Hong Zhao^a, Zhen Zhang^a, Dali Tan^a, Xinhe Bao^{a,*}

^a State Key Laboratory of Catalysis, Dalian Institute of Chemical Physics, Chinese Academy of Sciences, Dalian 116023, China

^b Hefei National Laboratory for Physical Sciences at the Microscale and Department of Chemical Physics, MPG-CAS Partner Group of Fritz-Haber-Institut der MPG, University of Science and Technology of China, Hefei 230026, China

Available online 14 January 2008

Abstract

A thin alumina film, the alumina model surfaces modified by the metallic molybdenum and by the MoO₃ are titrated by CO chemisorption. Two types of CO adsorption sites, namely octahedrally and tetrahedrally coordinated Al³⁺ sites, are present on the thin alumina film. The thin alumina film prepared under UHV conditions can be used to simulate the conventional high-surface-area alumina supports in real catalysis. The deposited metallic molybdenum preferentially occupies octahedrally coordinated Al³⁺ site and suppresses CO chemisorption on this site, and oxidation of the surface molybdenum species enhances this suppression.

© 2007 Published by Elsevier B.V.

Keywords: Preferential occupation; Molybdenum; Alumina; Thermal desorption spectroscopy

1. Introduction

The activation of methane to form desired commercial chemicals is a great challenge to catalysis science. Since Wang et al. of our laboratory first reported the dehydrogenation and aromatization of methane in the absence of oxygen on a transition metal ion-modified HZSM-5 zeolite catalyst in 1993 [1], the catalytic conversion of methane directly to aromatics in the absence of oxygen was extensively studied. Among the tested catalysts, Mo/HMCM-22 exhibits a good catalytic performance for this reaction [2]. Zeolite MCM-22 possesses a unique crystalline structure, combining the behavior of both the 10MR and 12MR systems [3]. It is well-known that the properties and the performance of zeolites usually depend on the state of the aluminum species in the zeolites, which plays a key role in catalytic reactions. The location of Al within the zeolite structure determines its function, for example, as Brønsted or Lewis acid sites [4–7]. Ammonia adsorption studies revealed that the observed Lewis acidity in the zeolite MCM-22 was derived from at least two types of framework aluminum sites (Al^F), that is, octahedral Al^F and three-

coordinate Al^F [8,9]. With Brønsted acid sites serving as a powerful trap, molybdenum migrated into the internal channels of the HMCM-22 zeolite and reacted preferentially with bridging hydroxyls groups [10]. It was established by NMR and DFT methods that strong interactions between guest and zeolite occurred in a Mo/HMCM-22 system, with the metal anchored to the tetrahedral Al^F through two oxygen bridges [11]. The location of the metal in turn modifies the acidic properties of the HMCM-22 and leads to a high dispersion of the molybdenum [10]. The synergic effect between molybdenum and Brønsted acid sites was considered to be the main reason for the outstanding catalytic performance of the 6Mo/HMCM-22 catalyst [12]. In light of the above description, a scientific question arises: why is the Mo primarily bonded to the tetrahedral Al^F, not to the octahedral Al^F?

In an attempt to investigate in detail the thermodynamic difference in the location of the molybdenum component on the tetrahedral Al³⁺ sites and on the octahedral Al³⁺ sites, a thin alumina film prepared in the ultrahigh-vacuum (UHV) system is chosen as the support for the molybdenum. Alumina has been applied widely as both catalysts and catalyst supports. While the oxygen ions form a closely packed and well-defined structure, the Al ions occupy the interstitial sites, forming the tetrahedral and/or octahedral aluminum sites. In the simplified bulk picture, the aluminum of amorphous Al₂O₃ is extensively

* Corresponding author. Tel.: +86 411 84686637; fax: +86 411 84691570.
E-mail address: xhbao@dicp.ac.cn (X. Bao).

tetrahedrally coordinated, while in α - Al_2O_3 the aluminum is extensively octahedrally coordinated. For γ - Al_2O_3 , θ - Al_2O_3 , β - Al_2O_3 , δ - Al_2O_3 and κ - Al_2O_3 , the aluminum ions occupy both tetrahedral and octahedral coordination sites. The key difference between these phases lies in the occupation probability of the tetrahedral and octahedral sites, therefore leading to differences in crystal structure and lattice constants [13]. The aluminum and oxygen ions are both coordinatively unsaturated on the surface, where aluminum cation functions as Lewis acid site and oxygen anion as Lewis base site. It has been shown that oxide films grown on the refractory metal substrates can successfully mimic the properties of the conventional high-surface-area oxides widely used as supports in real catalysis. This approach offers the advantage of using the full range of UHV surface analytical techniques to scrutinize the surface chemistry, while avoiding the charging problems that would normally occur when electron-based techniques are used with insulating samples. As a typical substrate, a thin Al_2O_3 film has been prepared and used to support the deposition of small metal aggregates [14–17].

In a preceding paper [18] a thin and fully dehydroxylated alumina film was fabricated as a catalyst support by deposition and oxidation of aluminum on a Pt(1 1 0) substrate in an oxygen ambient; then, metallic molybdenum was observed to be deposited on this alumina film via thermal decomposition of $\text{Mo}(\text{CO})_6$ and subsequent annealing at high temperatures. Molybdenum deposition on the thin Al_2O_3 film has also been achieved via thermal decomposition of $\text{Mo}(\text{CO})_6$ by Tysse and co-workers [19–22]. Metallic molybdenum or molybdenum oxide clusters supported on Al_2O_3 have widely been the subject of interest, and it has been well accepted that the role of Al_2O_3 , as a support, is not merely that of dispersing the clusters. The molecular structure and reactivity of the supported clusters have been intensively studied because of their importance in understanding the nature of the interaction between adsorbate and support and because of their important application in numerous catalytic reactions [23–25]. It is generally accepted that temperature-programmed methods, especially thermal desorption spectroscopy of carbon monoxide, are sensitive techniques for the investigation of adsorption sites on catalysts. In this study, the results of CO chemisorption on the thin alumina film, the alumina model surfaces modified by the metallic molybdenum and by the MoO_3 are reported. The results of CO desorption indicate that the metal preferentially occupies octahedrally coordinated Al^{3+} site, and the oxidation of the surface molybdenum intensifies this tendency of preferential occupation.

2. Experimental

Experiments were carried out in an UHV system with a base pressure of 2.0×10^{-10} mbar, which was described in detail elsewhere [18,26]. Briefly, the system was equipped with facilities for Auger electron spectroscopy (AES) and X-ray photoelectron spectroscopy (XPS), an ELS-22 instrument for high-resolution electron-energy-loss spectroscopy (HREELS), an ion gun for cleaning the sample, and a

quadrupole mass analyzer for verification of the purity of the inlet gas and the temperature-programmed desorption (TPD) experiments. A Pt(1 1 0) single crystal was fixed on the sample holder with Ta wires, and the temperature was monitored by a chromel–alumel thermocouple spot-welded on the back side of the sample. In the TPD experiments, the sample was heated at a rate of 8 K/s. In order to avoid the signal except from the front side of the sample, it was positioned at about 3 mm away from the collector of mass spectrometer. A homemade aluminum evaporator was used to prepare the thin Al_2O_3 film. The exposure was determined by integrating the pressure increase as a function of time, which was measured by an ion gauge without correction. All exposures determined in this way were specified hereafter as Langmuirs ($1 \text{ L} = 1.0 \times 10^{-6}$ Torr s).

3. Results

The thin alumina film on a Pt(1 1 0) substrate was prepared by deposition of aluminum in an oxygen ambient and then annealing up to 1200 K [18]. AES and XPS results indicated that the thin alumina film was essentially stoichiometric and fully covered the platinum substrate. The HREEL spectrum demonstrates three vibrational peaks at about 415 cm^{-1} , 658 cm^{-1} and 905 cm^{-1} on the thin alumina film, as also observed on the aluminum oxide surfaces on NiAl(1 1 0) and Ru(0 0 0 1) substrates [27]. Each of the three main loss features can be assigned to the octahedral and tetrahedral Al^{3+} occupation in crystalline Al_2O_3 films [28]. The appearance of three distinct vibrational features indicates that the thin oxide film has a long-range order. As pointed out, in situ UHV oxidation of Al single crystals showed markedly lower OH stability [29,30]. The thin oxide film is free from surface hydroxyl groups, as evidenced by HREELS. Thus, two different types of aluminum cations in octahedrally and tetrahedrally coordinated sites are present on the thin alumina film.

Coordinatively unsaturated (cus) aluminum sites, due to the absence of the surface hydroxyl groups, may provide opportunity for strong CO adsorption on the surface. CO chemisorption is carried out on this thin alumina film for characterization of these cus sites. Fig. 1 shows a series of thermal desorption spectra for 28 amu when the thin Al_2O_3 film was exposed to CO at room temperature. A desorption peak appears at approximately 500 K at low exposures. With the increased exposure to CO, this peak broadens and shifts toward lower temperature. At high exposures, the spectrum exhibits a growing asymmetry to higher temperature. At CO exposure of 15 L, the spectrum can be deconvolved into two components at approximately 395 K and 470 K, respectively.

Using $\text{Mo}(\text{CO})_6$ as a metal-containing precursor, molybdenum was deposited on the thin alumina film at 700 K under a $\text{Mo}(\text{CO})_6$ pressure of 5.0×10^{-7} Torr for 40 min. Fig. 2 displays TD spectra for 28 amu on the molybdenum model surfaces after exposure to 15 L CO. The sample is pre-heated for 3 min at 700 K, 800 K, 900 K, 1000 K, 1100 K and 1200 K, respectively. For the 700 K sample, the desorption signal

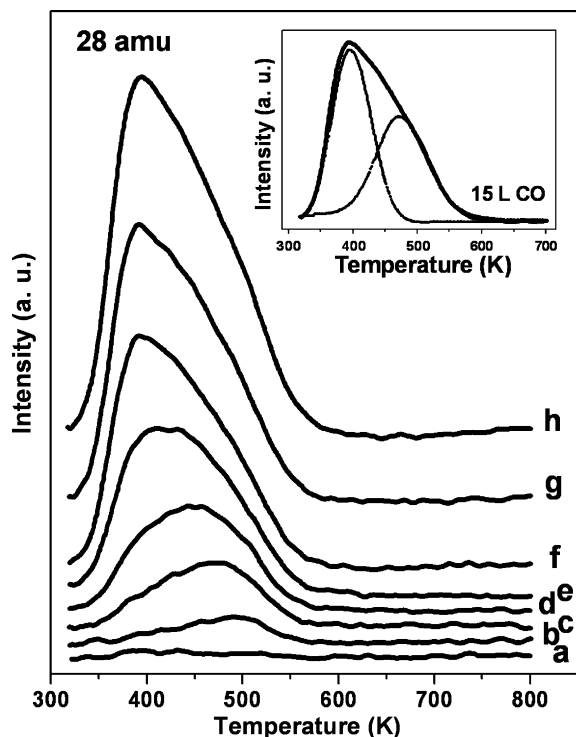


Fig. 1. TDS on the thin Al_2O_3 film with CO exposure of (a) 0 L, (b) 0.1 L, (c) 0.2 L, (d) 0.5 L, (e) 1 L, (f) 2 L, (g) 5 L and (h) 15 L, respectively.

exhibits a weak and broad peak at ~ 370 K. A new peak appears at ~ 330 K when the sample is pre-heated at 800 K. On the 900 K pre-heated sample, the new peak reaches its maximum, and the other at ~ 370 K increases in intensity. With continually

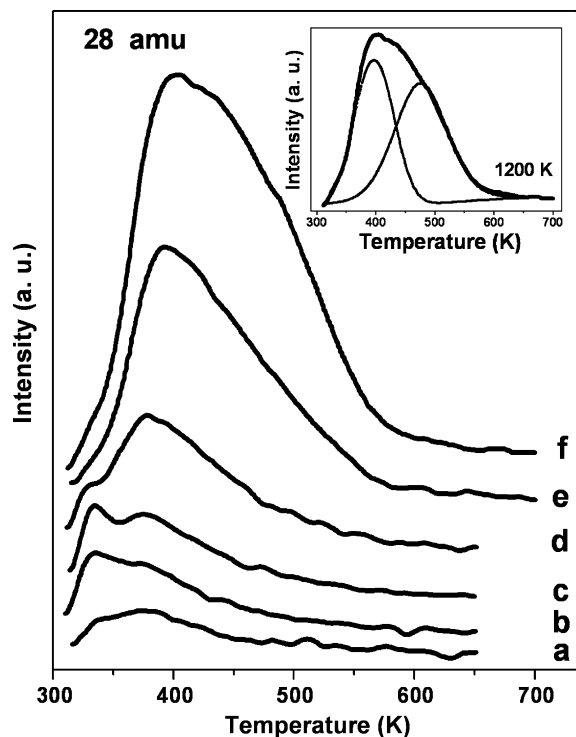


Fig. 2. TDS with CO exposure of 15 L on the surface of the molybdenum model surface annealed for 3 min at (a) 700 K, (b) 800 K, (c) 900 K, (d) 1000 K, (e) 1100 K and (f) 1200 K, respectively.

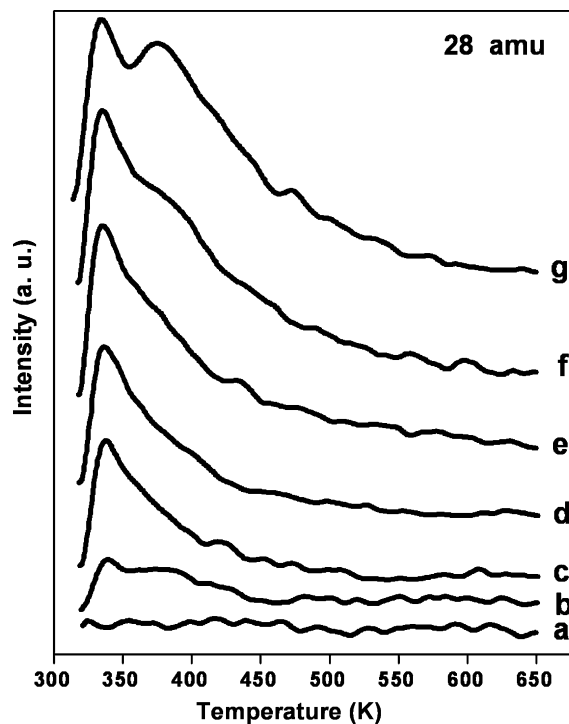


Fig. 3. TDS on the molybdenum model surface pre-heated at 900 K with CO exposure of (a) 0 L, (b) 0.2 L, (c) 0.5 L, (d) 1 L, (e) 2 L, (f) 5 L and (g) 15 L, respectively.

increasing the pre-heated temperature, the low-temperature peak loses its intensity, and the other increases in intensity and shifts toward higher temperature. The desorption peak at ca. 330 K disappears on the 1100 K pre-treated sample, and the other becomes obviously asymmetric to higher temperature. It is more asymmetric when the sample is pre-heated at 1200 K, and can be deconvoluted into two components at approximately 400 K and 475 K, respectively.

To distinctly reveal the desorption features of CO on these molybdenum model surfaces, two representative samples were chosen under 900 K and 1200 K pretreatment, respectively. Fig. 3 shows the CO TDS results for the sample pre-heated at 900 K for 3 min. A desorption peak appears at ~ 340 K at low CO exposures. With the increased exposure to CO, this peak increases in intensity and shifts toward lower temperature. While this peak eventually at ~ 330 K approaches to saturation, a new peak appears as a high-temperature tail. This new peak increases in intensity and shifts toward higher temperature with continually increasing CO exposure, finally settling at ~ 375 K with exposure to 15 L CO.

Fig. 4 displays the CO TDS results for the molybdenum model surface annealed at 1200 K for 3 min. A desorption peak appears at ~ 505 K at low CO exposures. With the increased CO exposure, this peak broadens and shifts toward lower temperature. The desorption spectrum exhibits two prominent peaks after exposure to 1 L CO, at ~ 415 K and ~ 485 K. With continually increasing CO exposure, the low-temperature peak shifts toward lower temperature and increases in intensity, while the other also slightly shifts downwards. At CO exposure of 15 L, the spectrum exhibits a prominent desorption feature at ~ 400 K, with a shoulder peak at ~ 475 K.

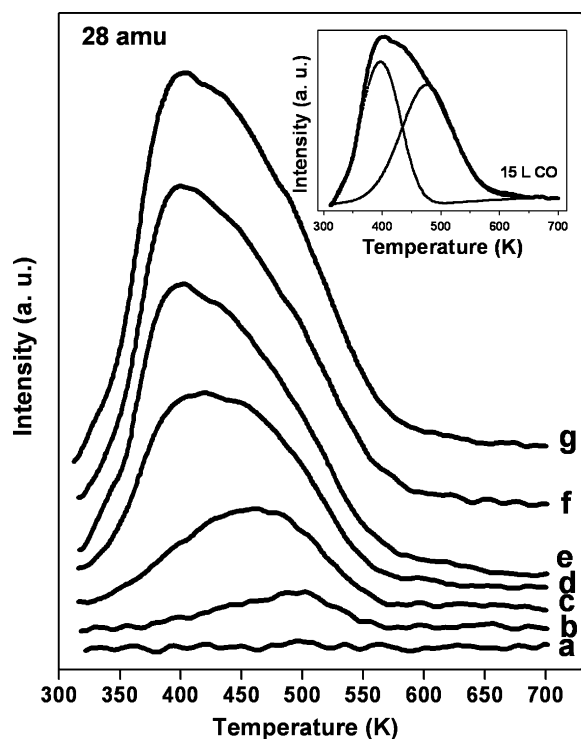


Fig. 4. TDS on the molybdenum model surface pre-heated at 1200 K with CO exposure of (a) 0 L, (b) 0.2 L, (c) 0.5 L, (d) 1 L, (e) 2 L, (f) 5 L and (g) 15 L, respectively.

After the molybdenum model surface was annealed at 1200 K, subsequent oxidation by NO_2 resulted in the alumina model surface modified by the MoO_3 , as evidenced by XPS (not shown in this paper). Then CO titration is carried out to monitor the adsorption sites on this model surface. As shown in Fig. 5, a desorption peak appears at ~ 520 K at low CO exposures. With the increased exposure to CO, this peak broadens and shifts toward lower temperature. At high exposures, this peak continually increases in intensity and shifts downwards, and a shoulder peak appears at a lower temperature. While the high-temperature peak eventually at ~ 480 K approaches to saturation, the low-temperature peak increases in intensity and gradually dominates with increasing CO exposure. At CO exposure of 15 L, the spectrum exhibits a prominent desorption feature at ~ 400 K, with a shoulder peak at ~ 480 K.

4. Discussion

Carbon monoxide can be used as a probe molecule to characterize the acidic and basic centers of the alumina support [31]. For each pair of OH groups removed by dehydroxylation, one Al^{3+} site is created on the surface and CO chemisorption can be formed on this site. CO desorption on the thin alumina film is distinguishable from that on the clean Pt(1 1 0) surface in both peak shape and position (see Fig. 6), indicating that CO desorption reliably comes from the thin alumina film. The alumina film has fully covered the platinum substrate, as evidenced by AES and XPS results [18]. The absence of a prominent CO desorption feature on the 700 K pre-heated sample, as shown in Fig. 2, further suggests that the CO

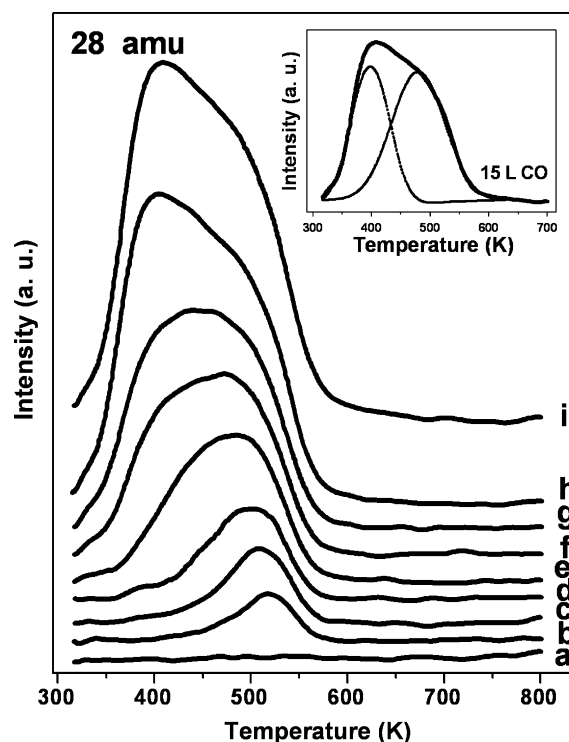


Fig. 5. TDS on the alumina model surface modified by the MoO_3 with CO exposure of (a) 0 L, (b) 0.1 L, (c) 0.2 L, (d) 0.3 L, (e) 0.5 L, (f) 1 L, (g) 2 L, (h) 7 L and (i) 15 L, respectively.

desorption signal comes from the thin alumina film, not from the back face of the platinum substrate. Cus aluminum sites may provide the adsorption sites for CO on the thin alumina film. However, no CO desorption was observed despite dosing the sample with up to 17 L CO even at liquid nitrogen temperature on $\gamma\text{-Al}_2\text{O}_3$, while a sharp CO desorption peak at 120 K and broader desorption peaks at 318 K and 395 K were observed on $\theta\text{-Al}_2\text{O}_3$; TDS of CO on $\alpha\text{-Al}_2\text{O}_3$ exhibited a prominent desorption peak at 120 K and a very broad peak at about 375 K [32]. In another case, TPD spectra of $\gamma\text{-Al}_2\text{O}_3$ exhibited only one desorption feature at 170 K [33,34]. CO was also usually used to probe the acidic center of $\gamma\text{-Al}_2\text{O}_3$ by volumetric and calorimetric studies even at room temperature [35]. No CO adsorption on the ordered Al_2O_3 film, which was prepared via oxidation of the clean NiAl(1 1 0) surface, was observed even at 90 K [36,37]. On a perfect alumina support, CO was detected to desorb in the temperature regime between 30 K and 70 K, according to the TDS results [14,38]. This weak interaction may be taken as an indication of an oxygen termination of the film, since stronger interaction could be expected in the presence of coordinatively unsaturated Al^{3+} ions [33]. Maybe our thin oxide film is not so perfect at the atomic level, that many coordinatively unsaturated Al^{3+} sites are exposed on the oxide surface, due to the surface defect. The thin alumina film, which is not so well-ordered as compared with the $\text{Al}_2\text{O}_3/\text{NiAl}(1\ 1\ 0)$ system [16,17], can probably be a better simulator for the realistic catalyst support. These Al^{3+} sites provide an opportunity for the strongly chemisorbed CO molecules on the thin Al_2O_3 film.

Carbonyl stretching frequencies of CO coordinated to cus cation sites on oxide surfaces are largely determined by the

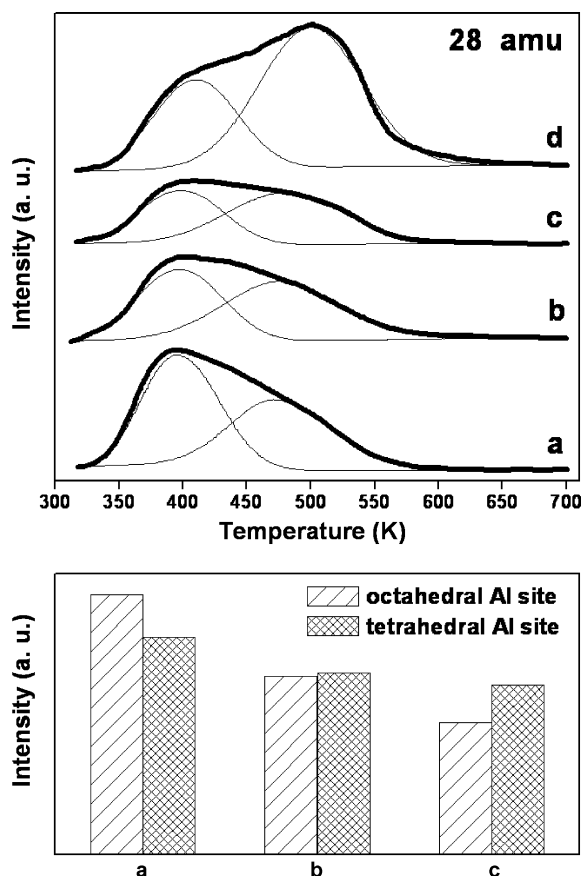


Fig. 6. TDS with CO exposure of 15 L on (a) the thin Al_2O_3 film, (b) the alumina model surface modified by the metallic molybdenum, (c) the alumina model surface modified by the MoO_3 and (d) the clean Pt(1 1 0) single crystal.

electric field strength produced by the cation sites. Al^{3+} site in tetrahedral coordination produces a stronger Lewis acid site than that in octahedral coordination. IR spectra of CO adsorbed on dehydroxylated Al^{3+} sites on the $\gamma\text{-Al}_2\text{O}_3$ surface were recorded in the CO stretch region, at 2195 cm^{-1} and 2226 cm^{-1} , respectively. The band at low vibrational frequency disappeared consequently upon degassing for a while, whereas the other was removed at a relatively higher temperature [39]. The former was assigned to CO species bound on octahedral Al^{3+} sites and the latter to CO species bound on tetrahedral Al^{3+} sites [40]. Accordingly, in the CO desorption spectra on our alumina film, the low-temperature peak is assigned to CO chemisorption on octahedral Al^{3+} sites, and the other to CO on tetrahedral Al^{3+} sites. Unfortunately, due to the interference from the strong phonon losses of the alumina substrates, CO stretching frequencies were not detected by HREELS.

Molybdenum atoms are deposited via thermal decomposition of $\text{Mo}(\text{CO})_6$ at the substrate temperature of 700 K, simultaneously with some surface carbon residual on the surface [18]. These atoms cover nearly all the adsorption sites of CO, inducing that the desorption signal of CO exhibits a weak and broad peak at $\sim 370\text{ K}$. With increasing sample temperature, the surface molybdenum atoms agglomerate into clusters and the surface carbon atoms form carbide species with molybdenum. AES and XPS measurements also revealed that a

monolayer of molybdenum carbide was deposited onto the alumina surface after $\text{Mo}(\text{CO})_6$ exposure of $\sim 40\text{ L}$ [41]. Mo metal dissociates CO effectively; only for high exposures, where dissociated CO was saturated, was molecularly adsorbed CO observed at about 310 K [42]. Whereas, CO desorption spectrum on $\alpha\text{-Mo}_2\text{C}$ (0 0 0 1) surface exhibited a relatively symmetric peak, which shifted toward lower temperature with increasing CO exposure, from 440 K at 0.03 L to 345 K at a saturation exposure of 0.38 L [43]. Thus, the peak at approximately 330 K in Fig. 2 is attributed to CO desorption from the surface molybdenum carbide species, rather than from the metallic molybdenum clusters. The lower temperature of CO desorption features on the 800 K pre-heated sample, as compared with that on $\alpha\text{-Mo}_2\text{C}$ (0 0 0 1) surface, is probably due to the electron-deficiency of the surface molybdenum carbide species, which is caused by the electron transfer from the deposited clusters to the alumina substrate. On the 900 K pre-heated sample, much of the surface carbon atoms form carbide, and molybdenum atoms on the surface continually aggregate, exposing a portion of the alumina surface. With continually increasing sample temperature, molybdenum carbide species starts to be reduced by reaction with the oxygen contained in the oxide substrate, and molybdenum clusters keep on agglomerating on the surface, exposing more part of the thin alumina surface. The reduction of the molybdenum carbide species was also observed by heating at high temperatures in literature [41]. These changes result in the loss of intensity for the desorption peak at ca. 330 K, and the intensity growth of the other peak which in the meantime shifts toward higher temperature. When the molybdenum model surface is pre-heated at 1100 K, the disappearance of the desorption signal at ca. 330 K further confirms that this CO desorption signal does not come from the surface molybdenum clusters, and suggests that the surface molybdenum carbide species has been completely reduced at this annealing temperature. For the 1200 K sample, the surface molybdenum increases its agglomeration, exposing most of the alumina surface. However, no Mo 3d signal related to the molybdenum carbide species is detected on the surface during the whole annealing process by XPS (not shown), probably because of the little amount of the formed carbide. The molybdenum carbide was formed on the topmost layer of the molybdenum clusters. On the one hand, this distribution of the molybdenum carbide leads to comparatively intense CO desorption features from the 800 K and 900 K samples; on the other hand, the relatively little amount of the molybdenum carbide can not be detected by XPS. After heated to 1200 K, no signal of Mo 3d correlated with oxidized species can be observed. It is also thermodynamically evidenced that the surface molybdenum species cannot be oxidized by the oxygen from the Al_2O_3 film upon 1200 K annealing, and still maintains its metallic nature [44]. The peak at $\sim 400\text{ K}$ is also assigned to CO desorption from octahedrally coordinated Al^{3+} sites, and the other to CO desorption from tetrahedrally coordinated Al^{3+} sites. Although desorbing at a lower temperature, CO still preferentially chemisorbs on the surface molybdenum carbide species, as observed in Fig. 3 as a function of CO exposure.

There was negligible adsorption of CO on the MoO₃ under UHV conditions following dehydroxylation at 1200 K and dosing with an equilibrium pressure of 5.0 Torr of CO at 140 K probed by IR spectra [34]. Therefore, the surface MoO₃ species needs not to be taken into consideration for CO chemisorption at room temperature. Then on the alumina model surface modified by the MoO₃, the low-temperature peak is likewise assigned to CO desorption from octahedrally coordinated Al³⁺ sites, and the other to CO desorption from tetrahedrally coordinated Al³⁺ sites.

For quantitative comparison, Fig. 6 displays the desorption features of CO with 15 L exposure on the thin Al₂O₃ film, the alumina model surfaces modified by the metallic molybdenum and by the MoO₃, respectively. CO desorption on a clean Pt(1 1 0) surface is also shown on the top of this figure. The desorption temperature and the peak shape of CO on the Pt(1 1 0) surface are quite different from those of CO on the three model surfaces, whereas the desorption intensities are of the same order of magnitude. These results illustrate that in the case of three model surfaces CO desorption trustworthily comes from the surfaces, but not from the back face of the Pt substrate, since the Pt(1 1 0) front face has already been fully covered with the alumina film as evidenced by AES and XPS [18]. The desorption features on the three model surfaces were deconvolved into two separate peaks shown in the upper panel, a low-temperature component and a high-temperature component, corresponding to CO desorption from octahedrally and tetrahedrally coordinated Al³⁺ sites, respectively. The desorption intensities of CO on these model surfaces are also shown in the bottom panel. It can be seen that, in the sequence of the thin alumina film, the alumina surfaces modified by the metallic molybdenum and by the MoO₃, the desorption component from octahedrally coordinated Al³⁺ sites markedly loses its intensity while the other slightly decreases, and they both slightly shift toward higher temperature. The upward shifts in the desorption temperatures of these two components are due to the modification of the thin Al₂O₃ film induced by the surface clusters. The thin Al₂O₃ film grows electron-rich due to the deposition of these surface clusters, and this electron sufficiency of the substrate increases the back-donation to the adsorbed CO species, which grows more stable on the modified surface.

The preferential occupation of the octahedral or tetrahedral vacant sites available on the Al₂O₃ surface by the dispersed species is related to the intrinsic properties and the amount of the surface species, as well as the calcination temperature used for sample preparation. On the thin alumina surface modified by the metallic molybdenum, the CO desorption peak from octahedrally coordinated Al³⁺ sites obviously loses intensity in comparison with that on the thin alumina film, while the peak from tetrahedrally coordinated Al³⁺ sites slightly decreases. This illuminates that the deposited molybdenum preferentially occupies octahedrally coordinated Al³⁺ site, indicating a physically site-blocking effect and the suppression for CO chemisorption on the alumina surface. TDS results of CO on the molybdenum model surfaces pre-heated at various temperatures indicate that this suppression is enhanced with the

coverage of the surface species. With increasing sample temperature, molybdenum aggregates on the surface and the underlying Al₂O₃ surface is gradually exposed, consequently CO desorption increases in intensity. When the surface metallic molybdenum is oxidized into the MoO₃, molybdenum oxide spreads over the surface of the thin alumina film. In earlier experiments an almost unrestricted spreading of the supported molybdates uncovered only undetectably small parts of the support surface [39,45]. Again laser Raman spectroscopy investigation [46] and IR and TPD measurements [34] of MoO₃/Al₂O₃ catalysts indicated that under dehydrating conditions polymeric molybdate species spread to form octahedrally coordinated MoO₃ units on the surface of γ -Al₂O₃. In recent studies on silica support [47] and on alumina model supports [48,49] spreading of MoO₃ was also observed. After thermal treatment, MoO₃ formed a monolayer or a submonolayer on the flat surface of the stable Al₂O₃ and SiO₂ thin films. Spreading of molybdenum oxide causes more portions of the octahedral Al³⁺ sites to be covered, hence hindering CO chemisorption on these Al³⁺ sites. Therefore, the CO desorption intensity from the alumina model surface modified by the MoO₃ is further decreased, as compared with that from the alumina model surface modified by the metallic molybdenum.

On the thin alumina film prepared under UHV conditions, the metallic molybdenum and the MoO₃ both preferentially occupy the octahedrally coordinated Al³⁺ sites. No spatial restriction exists on the oxide substrate for the location of the metallic molybdenum and the MoO₃. It is thermodynamically dominated for the preferential occupation on the octahedral Al³⁺ sites of the molybdenum species. However, the active molybdenum species is anchored to the tetrahedral framework aluminum sites in the internal channel of the HMCM-22 zeolite through two oxygen bridges [11]. Besides the thermodynamic factor, the steric restriction of the internal channel of the HMCM-22 zeolite must be taken into consideration, and it can play a very important role in the location of the molybdenum species on the HMCM-22 zeolite. The MCM-22 zeolite has two types of pore systems, one is 10MR two-dimensional sinusoidal channels and the other is 12MR supercages with a depth of 18.2 Å, both accessible through 10MR windows [3,50,51]. The molybdenum species are stabilized on the HMCM-22 zeolite, via the steric confinement by the internal channels with certain diameters. Additionally, it is more important that in real zeolite catalysts the alumina surface has abundant hydroxyl groups and exposes many Brønsted acid sites, while the alumina film prepared in the UHV system has lower OH stability. With Brønsted acid sites serving as a powerful trap, molybdenum migrated into the internal channels of the HMCM-22 zeolite and reacted preferentially with bridging hydroxyls groups [10]. Strong interactions between the molybdenum species and Brønsted acid sites have been already confirmed by NMR and DFT methods [11]. Under the combinatorial effects of the acidity and the steric restriction, the location of the molybdenum species on the tetrahedral Al³⁺ sites is more stable than that on the octahedral Al³⁺ sites, where the molybdenum species are bound to the tetrahedrally coordinated

Al³⁺ sites through oxygen bridges [11]. Experimentally, the dealumination of zeolite plays a key role in the catalyst preparation [52]. It may not only change the strength and the amount of the Brønsted acidity, but also slightly modify the steric shape of the internal channel of the HMCM-22 zeolite [9]. From a thermodynamic point of view, the thin alumina film prepared under UHV conditions can be a good simulator for the real catalyst carriers. However, the great differences still exist between the alumina surface and the real catalyst carriers, such as the surface hydroxyl groups and the Brønsted acidity. In this respect, the surface hydroxyl groups should be further investigated in detail and systematically on the ordered oxide film under UHV conditions.

5. Conclusions

In summary, the thin alumina film is prepared as the catalyst substrate under UHV conditions, and the alumina model surfaces modified by the metallic molybdenum and by the MoO₃ are also prepared. HREELS and CO desorption results indicate that two types of CO adsorption sites are present on the thin alumina film, namely octahedrally and tetrahedrally coordinated Al³⁺ sites. The low-temperature component in CO desorption spectra is attributed to CO desorption from octahedrally coordinated Al³⁺ site, and the other from tetrahedrally coordinated Al³⁺ site. The metallic molybdenum and molybdenum oxide preferentially inhabit octahedrally coordinated Al³⁺ sites on the alumina film, and remarkably suppress CO chemisorption on these Al³⁺ sites. Oxidation causes the deposited species to spread over the surface, which reduces the CO desorption intensity from octahedrally coordinated Al³⁺ sites more than that on the alumina model catalyst modified by the metallic molybdenum.

Acknowledgements

We are grateful for the financial support of the National Natural Science Foundation of China and the Ministry of Science and Technology of China.

References

- [1] L.S. Wang, L.X. Tao, M.S. Xie, G.F. Xu, J.S. Huang, Y.D. Xu, *Catal. Lett.* 21 (1993) 35.
- [2] Y.Y. Shu, D. Ma, L.Y. Xu, Y.D. Xu, X.H. Bao, *Catal. Lett.* 70 (2000) 67.
- [3] M.E. Leonowicz, J.A. Lawton, S.L. Lawton, M.K. Rubin, *Science* 264 (1994) 1910.
- [4] J. Rocha, S.W. Carr, J. Klinowski, *Chem. Phys. Lett.* 187 (1991) 401.
- [5] L. Kellberg, M. Linsten, H.J. Jakobsen, *Chem. Phys. Lett.* 182 (1991) 120.
- [6] F. Deng, Y.R. Du, C.H. Ye, J.Z. Wang, T.T. Ding, H.X. Li, *J. Phys. Chem.* 99 (1995) 15208.
- [7] L.C. de Ménorval, W. Buckermann, F. Figueras, F. Fajula, *J. Phys. Chem.* 100 (1996) 465.
- [8] D. Ma, X.W. Han, S.J. Xie, X.H. Bao, H.B. Hu, S.C.F. Au-Yeung, *Chem. Eur. J.* 8 (2002) 162.
- [9] D. Ma, F. Deng, R.Q. Fu, X.W. Han, X.H. Bao, *J. Phys. Chem. B* 105 (2001) 1770.
- [10] D. Ma, Y.Y. Shu, X.W. Han, X.M. Liu, Y.D. Xu, X.H. Bao, *J. Phys. Chem. B* 105 (2001) 1786.
- [11] D. Ma, X.W. Han, D.H. Zhou, Z.M. Yan, R.Q. Fu, Y.D. Xu, X.H. Bao, H.B. Hu, S.C.F. Au-Yeung, *Chem. Eur. J.* 8 (2002) 4557.
- [12] D. Ma, Q.J. Zhu, Z.L. Wu, D.H. Zhou, Y.Y. Shu, Q. Xin, Y.D. Xu, X.H. Bao, *Phys. Chem. Chem. Phys.* 7 (2005) 3102.
- [13] P. Gassmann, R. Franchy, H. Ibach, *Surf. Sci.* 319 (1994) 95.
- [14] M. Bäumer, H.-J. Freund, *Prog. Surf. Sci.* 61 (1999) 127.
- [15] H.-J. Freund, M. Bäumer, J. Libuda, T. Risse, G. Rupprechter, S. Shai-khutdinov, *J. Catal.* 216 (2003) 223.
- [16] G. Ceballos, Z. Song, J.I. Pascual, H.-P. Rust, H. Conrad, M. Bäumer, H.-J. Freund, *Chem. Phys. Lett.* 359 (2002) 41.
- [17] M. Kulawik, N. Nilius, H.-P. Rust, H.-J. Freund, *Phys. Rev. Lett.* 91 (2003) 256101.
- [18] Z.Q. Jiang, W.X. Huang, J. Jiao, H. Zhao, D.L. Tan, R.S. Zhai, X.H. Bao, *Appl. Surf. Sci.* 229 (2004) 43.
- [19] M. Kaltchev, W.T. Tysoc, *J. Catal.* 193 (2000) 29.
- [20] Y. Wang, F. Gao, M. Kaltchev, D. Stacchiola, W.T. Tysoc, *Catal. Lett.* 91 (2003) 83.
- [21] Y. Wang, F. Gao, W.T. Tysoc, *J. Mol. Catal. A* 236 (2005) 18.
- [22] Y. Wang, F. Gao, W.T. Tysoc, *J. Mol. Catal. A* 248 (2006) 32.
- [23] G. Mestl, N.F.D. Verbruggen, F.C. Lange, B. Tesche, H. Knözinger, *Langmuir* 12 (1996) 1817.
- [24] I.E. Wachs, *Catal. Today* 27 (1996) 437.
- [25] S. Andersson, P.A. Brühwiler, A. Sandell, M. Frank, J. Libuda, A. Giertz, B. Brena, A.J. Maxwell, M. Bäumer, H.-J. Freund, N. Märtensson, *Surf. Sci.* 442 (1999) L964.
- [26] Z.Q. Jiang, H. Zhao, D.L. Tan, R.S. Zhai, X.H. Bao, *Chin. J. Catal.* 26 (2005) 423.
- [27] M.B. Lee, J.H. Lee, B.G. Frederick, N.V. Richardson, *Surf. Sci.* 448 (2000) L207.
- [28] Z.Q. Jiang, W.X. Huang, Z. Zhang, H. Zhao, D.L. Tan, X.H. Bao, *Surf. Sci.* 601 (2007) 844.
- [29] J.G. Chen, P. Basu, L. Ng, J.T. Yates, *Surf. Sci.* 194 (1988) 397.
- [30] J.E. Crowell, J.G. Chen, D.M. Hercules, J.T. Yates, *J. Chem. Phys.* 86 (1987) 5804.
- [31] C. Morterra, G. Magnacca, G. Cerrato, N. Del Favero, F. Filippi, C.V. Folonari, *J. Chem. Soc. Faraday Trans.* 1 89 (1993) 135.
- [32] G.S. Hsiao, W. Erley, H. Ibach, *Surf. Sci.* 405 (1998) L465.
- [33] A.L. Diaz, W.W.C. Quigley, H.D. Yamamoto, M.E. Bussell, *Langmuir* 10 (1994) 1461.
- [34] A.L. Diaz, M.E. Bussell, *J. Phys. Chem.* 97 (1993) 470.
- [35] M.C. Machado, J.M. Guil, A.P. Masiá, A.R. Paniego, J.M.T. Menayo, *Langmuir* 10 (1994) 685.
- [36] J. Libuda, A. Sandell, M. Bäumer, H.-J. Freund, *Chem. Phys. Lett.* 240 (1995) 429.
- [37] A. Sandell, J. Libuda, M. Bäumer, H.-J. Freund, *Surf. Sci.* 346 (1996) 108.
- [38] R.M. Jaeger, J. Libuda, M. Bäumer, K. Homann, H. Kuhlenbeck, H.-J. Freund, *J. Electron Spectrosc. Relat. Phenom.* 64/65 (1993) 217.
- [39] M.I. Zaki, B. Vielhaber, H. Knözinger, *J. Phys. Chem.* 90 (1986) 3176.
- [40] M.I. Zaki, H. Knözinger, *Spectrochim. Acta* 43A (1987) 1455.
- [41] M. Kaltchev, W.T. Tysoc, *J. Catal.* 196 (2000) 40.
- [42] K.-I. Fukui, T. Aruga, Y. Iwasawa, *Surf. Sci.* 281 (1993) 241.
- [43] T.P. St. Clair, S.T. Oyama, D.F. Cox, *Surf. Sci.* 468 (2000) 62.
- [44] Z.Q. Jiang, W.X. Huang, Z. Zhang, H. Zhao, D.L. Tan, X.H. Bao, *Chem. Phys. Lett.* 439 (2007) 313.
- [45] J. Leyrer, B. Vielhaber, M.I. Zaki, S. Zhuang, J. Weitkamp, H. Knözinger, *Mater. Chem. Phys.* 13 (1985) 301.
- [46] C.C. Williams, J.G. Ekerdt, J.-M. Jehng, F.D. Hardcastle, I.E. Wachs, *J. Phys. Chem.* 95 (1991) 8791.
- [47] S. Braun, L.G. Appel, V.L. Camorim, M. Schmal, *J. Phys. Chem. B* 104 (2000) 6584.
- [48] S. Günther, M. Marsi, A. Kolmakov, M. Kiskinova, M. Noeske, E. Taglauer, G. Mestl, U.A. Schubert, H. Knözinger, *J. Phys. Chem. B* 101 (1997) 10004.
- [49] G. Mestl, H. Knözinger, *Langmuir* 14 (1998) 3964.
- [50] S. Nicolopoulos, J.M. González-Calbet, M. Vallet-Regí, A. Corma, C. Corell, J.M. Guil, J. Pérez-Pariante, *J. Am. Chem. Soc.* 117 (1995) 8947.
- [51] A. Corma, *Microporous Mesoporous Mater.* 21 (1998) 487.
- [52] D. Ma, Y. Lu, L.L. Su, Z.S. Xu, Z.J. Tian, Y.D. Xu, L.W. Lin, X.H. Bao, *J. Phys. Chem. B* 106 (2002) 8524.